

INCREASING THE FLUX OF A THOMSON SOURCE WHILE MAINTAINING A NARROW BANDWIDTH BY USING LARGE ENERGY SPREAD PRIMARY PARTICLES

M. Ruijter¹*, A. Bacci¹, I. Drebot¹, M. Opromolla³, V. Petrillo²,
M. Rossetti Conti¹, A. R. Rossi¹, S. Samsam¹, L. Serafini¹

¹ INFN-Milano, Milan, Italy

² Università degli Studi di Milano, Milan, Italy

³ INFN-LNF, Frascati, Italy

Abstract

Thomson/Compton scattering is a method to produce high energy photons through the collision of low energy photons in a laser pulse onto relativistic electrons. In the linear (incoherent) Thomson/Compton regime, the flux scales linearly with the number of primary particles and the bandwidth of the produced photons depend, amongst other factors, on the energy spread of them. In general, an increase of the primary particles is connected to a larger energy spread (e.g. non-constant acceleration gradients, collective effects, etc). Therefore their number is restricted by the desired bandwidth, and thus limits the flux. In our previous (theoretical) studies we showed that the ideal Thomson spectrum can be retrieved when an electron bunch with a linear energy correlation of several percent collides with a matched linearly chirped laser pulse.

Here we extend the scheme to allow for higher order energy correlations and quantify how the electron distribution influences the bandwidth. Furthermore we discuss the practical viability to maximize the primary particles, with the focus on linear accelerators (LINACS) for the electrons and laser pulses based on the chirped pulse amplification (CPA) scheme. These could potentially provide up to tens of nano-Coulomb electron bunches and tens, or even over a hundred, Joule lasers pulses respectively.

INTRODUCTION

High energy photons, i.e. keV-MeV, allow for higher resolution imaging [1, 2] and is used for material science or medical applications [3], and allows for the study of physical phenomena such as nuclear photonics [4]. Thomson scattering is a method to generate these photons by colliding highly relativistic electrons on an intense laser pulse. Experimentally this type of source has gained attention for two reasons: 1) because of the lower energy requirement on the electrons, as compared to undulators/FELs, which reduces the size of machinery, and moreover 2) the reduction in costs of high energy density laser pulses operating at high repetition rate. Current designs rely on maintaining the narrow bandwidth by using (close to) ideal initial particles [5].

On the theoretical front many methods are being explored in order to increase the number of (generated) photons, while

maintaining a high quality source. Several studies focus on the compensation of the non-linear broadening due to the intensity of the laser (meaning the amplitude of the normalized vector potential $a_0 = \frac{eA_0}{mc^2} \geq 1$) which can be categorized into using a chirped laser pulse [6] and polarization gating [7]. Others have investigated the use of the non-linear broadening to compensate for the energy spread of electrons [8]. In the linear Thomson regime ($a_0 \ll 1$) studies have been put forward on preparing the electron bunch, monochromatically [9] and with energy spread [10], in such a way to increase the coherency of the radiation they emit. In our previous studies [11, 12] we showed that preserving the monochromatic (incoherent) Thomson spectrum while utilizing large energy spread electrons with a chirped laser pulse is possible. In this work we extend the study of the geometry where the energy correlation is along the propagation direction of the electrons, as depicted in Fig. 1. The relation for the instantaneous laser frequency and phase were found to be

$$\frac{\omega_l(\zeta)}{c} \equiv \frac{\partial \eta}{\partial \zeta} = \left(\frac{\langle \gamma \rangle}{\gamma \left(\frac{1+\beta}{\beta} z \right)} \right)^2 \frac{\omega_{l,0}}{c}, \quad (1)$$

$$\eta \approx \frac{\omega_l(\zeta)}{c} \zeta, \quad (2)$$

where γ is the Lorentz factor of the electron, β the velocity normalized to the speed of light c , $\zeta = \frac{\omega_{l,0}}{c}(ct - z)$ the unchirped laser phase with $\omega_{l,0}$ the central laser frequency.

For this geometry the primary beams need to collide under an angle, and on top need to have a sufficiently small energy gradient, in order for the correct frequency-energy matching to occur. Thus a bunch with a large energy spread needs to be long. This in fact means that electron bunches obtained using plasma based acceleration schemes are not a viable option as the energy gradient is too large. However, for the traditional linear accelerators the requirement of a long bunch is beneficial for the Thomson scheme: as was shown in [13] 1) the long bunch reduces space-charge forces 2) allows for much larger bunch charge, of several nano Coulombs [14–17]. 3) the energy spread of the electrons and its correlation is controllable. The dynamics of transporting large energy spread bunches have been studied in detail in Refs. [18, 19] for a similar concept: the Transverse gradient undulator.

* marcel.ruijter@mi.infn.it

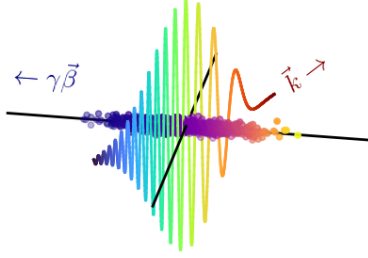


Figure 1: Schematic overview for the energy compensation Thomson Scattering Scheme. The electron bunch has an energy-position correlation along its propagation direction that is matched to with a frequency within the laser pulse. The produced radiation will be centered around the ideal Thomson frequency.

Laser systems required for this application are readily available, even on the commercial level [20]; Joule class chirped pulse amplified laser pulses [21]. In principle the laser system could be designed such that the Thomson interaction point lies within an amplification stage to maintain the pulse energy. This potentially would lead to higher repetition rate for the source and, moreover, the energy consumption would decrease twofold; first the same pulse is being used and second there is no need for compression that have losses of about 25-30 %.

Various experiments have shown that the control higher order dispersion can be controlled to high degree of precision with high intensity laser pulses [22–24].

METHODS

The Thomson spectrum is calculated as the sum of N_e incoherent (macro) particles in the far field though the, on the Lienard Wiechert potentials based, double differential equation

$$\frac{d^2 N_x}{d\omega d\Omega} = \sum_{n=1}^{N_e} \frac{\omega}{\hbar c} \left(\frac{e}{2\pi} \right)^2 \left| \int_{-\infty}^{\infty} dt \hat{n} \times \hat{n} \times \vec{\beta}_n \exp\left[i \frac{\omega}{c} (ct - \hat{n} \cdot \vec{r}_n) \right] \right|^2, \quad (3)$$

where \hat{n} is the unit vector to an observation point on a spherical surface, \vec{r}_n and $\vec{\beta}_n$ are the trajectory and velocity of a macro particle. The particle trajectories are obtained by using a 3D Lorentz force particle tracker. The detector works as a numerical aperture and has a maximum azimuthal angle of $\vartheta_{max} = \frac{1}{6\gamma}$ to maintain a semi-symmetric spectral envelope shape [25]. Increasing the acceptance angle further does increase the number of photons collected, however their energy will be lower due to the energy-angular dependency ($\omega(\vartheta) \propto \frac{1}{1+\gamma^2\vartheta^2}$).

Electron Bunch Parameters

Electron bunches are generally modeled and characterized through variances of the phase space coordinates or combined into a covariance matrix. Here we assume that the transverse and longitudinal phase space are uncoupled. This means that the longitudinal covariance matrix is given by

$$M_{z,\epsilon} = \begin{bmatrix} \langle z^2 \rangle & \langle z\gamma\beta_z \rangle \\ \langle z\gamma\beta_z \rangle & \langle (\gamma\beta_z)^2 \rangle \end{bmatrix}. \quad (4)$$

The determinant of this matrix gives the longitudinal emittance. The term $\langle z\gamma\beta_z \rangle$ can be expressed in as the product of $\langle z^2 \rangle \langle (\gamma\beta_z)^2 \rangle \alpha_\epsilon$. The parameter $-1 \leq \alpha_\epsilon \leq 1$ then controls the direction of the slope and the amount of correlation ($|1|$ fully correlated & 0 fully uncorrelated). Per definition this distribution can at most have a linear correlation ($\gamma(z) = \frac{\langle (\gamma\beta_z)^2 \rangle}{\langle z^2 \rangle} z + \langle \gamma \rangle$, see left panel of Fig. 2). To explore the possibility and dynamics of the compensation of higher order energy correlation we transform the linear energy to a quadratic using $\gamma(z) = A_e z^2 + B_e z + C_e$ for each particle, such that the average and energy spread remain equal. The electron bunches generated for the simulations, see Fig. 2, share similar characteristics as studied in Refs. [13, 26], where they were obtained from beam dynamics simulations.

Laser Pulse

The instantaneous frequency of the laser pulse should change slowly, as we want a single frequency in the interaction region. Therefore the laser phase can be approximated with the slowly varying amplitude approximation to give [11]

$$\eta(\zeta) \approx A_\omega \zeta^2 + B_\omega \zeta + C_\omega. \quad (5)$$

The coefficients will depend on the electron energy correlation according to Eq. (1). To denote the chirp order (ηO) we will use 0 for unchirped ($\eta = \zeta$), linear 1 and quadratic chirp 2. Like in our previous study we use two Gaussian beams that intersect at the interaction region. The longitudinal profile is rectangular (flat-top).

RESULTS

Additional parameters for the simulation results in Figs. 3 and 4 are: the electron distribution has a charge of 1 nC, a transverse emittance of 1 mm rad with rms spot size of 15 μm , the laser is linearly polarized and has a waist of $W_0 = 20 \mu\text{m}$. The two beams collide at an angle of 52° , leading to an interaction length of 100 μm as in Ref. [11].

Figure 3 shows a quadratic chirp is beneficial for a strong quadratic correlation and high α_ϵ (meaning low uncorrelated energy spread). When increasing the energy spread we see an increase in N_x , as is shown in Fig. 4, which is the consequence of having particles with higher energy than in the other distributions in combination with the lower frequency photons (i.e more laser photons in that section of the laser pulse to scatter with). Since we are still in the linear regime N_x increases with the intensity of the laser as expected.

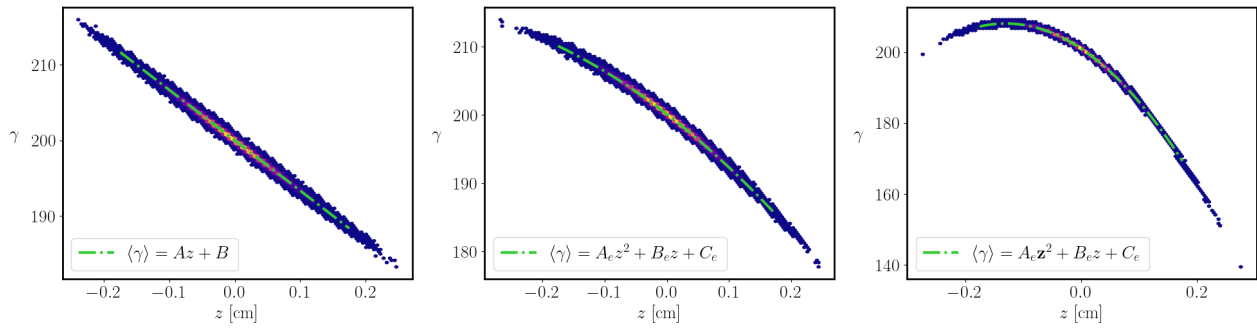


Figure 2: Electron distributions with an energy-position correlation along its propagation direction ($-\hat{z}$). For all cases $\sigma_\gamma = 0.016$ (2.7 %), $\sigma_\gamma \beta_z = 3.33$ and $\alpha_\epsilon = 0.996$. Left: Linear correlation as can be obtain by a 6D Gaussian covariance matrix. Middle: bunch transformed to have weak quadratic energy correlation ($A_e = -76.19$, $B_e = -70.47$, $C_e = 200.1$) and Right: with strong quadratic signature ($A_e = -416.66$, $B_e = -108.33$, $C_e = 201$).

For a laser pulse with an amplitude of $a_0 = 5 \cdot 10^{-2}$ and quadratic chirp ($A_\omega = 3.4 \cdot 10^{-10}$, $B_\omega = 9 \cdot 10^{-6}$, $C_\omega = .99$) the number of photons that pass through the (numerical) aperture are $N_x = 2.9 \cdot 10^8$ within a bandwidth of $\frac{\sigma_\omega}{\omega} = 0.017$.

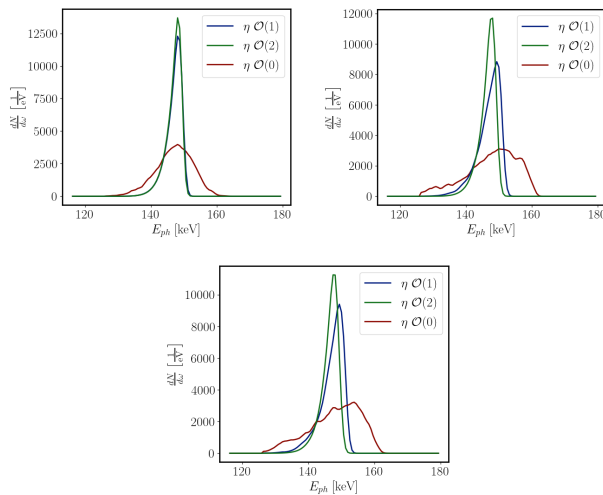


Figure 3: Spectra for (red) unchirped, (blue) linearly chirped and (green) quadratic chirped laser pulse for three different electron bunch distributions with a bunch charge of $Q = 1$ nC and $\sigma_\gamma = 2.7$ %, and a laser amplitude of $a_0 = 10^{-2}$. Left: $\alpha_\epsilon = 0.996$ and quadratic relation ($A_e = -76.19$, $B_e = -70.47$, $C_e = 200.1$) Middle: $\alpha_\epsilon = 0.9998$ and quadratic relation ($A_e = -416.66$, $B_e = -108.33$, $C_e = 201$) Right: $\alpha_\epsilon = 0.996$ and quadratic relation ($A_e = -416.66$, $B_e = -108.33$, $C_e = 201$).

Improvements on the photon number can be achieved mainly by increasing the bunch charge, as with $a_0 = 5 \cdot 10^{-2}$ we are already close to the non-linear regime. For example, if the bunch charge were 5 nC with an $\alpha_\epsilon = 0.9998$ the N_x would be a factor 6 higher and therefore reach up to $10^9 - 10^{10}$ per shot.

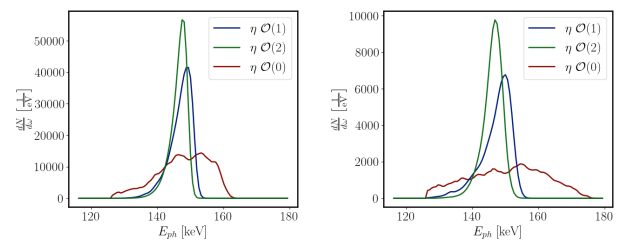


Figure 4: Spectra for (red) unchirped, (blue) linearly chirped and (green) quadratic chirped laser pulse for two different electron bunch distributions with a bunch charge of $Q = 1$ nC and $\alpha_\epsilon = 0.996$. Left: $\sigma_\gamma = 2.7$ % and $a_0 = 5 \cdot 10^{-2}$ Right: $\sigma_\gamma = 4.8$ % and $a_0 = 1 \cdot 10^{-2}$.

CONCLUSION

We showed that the ideal Thomson spectrum can be obtained with an electron bunch with a higher order correlated energy spread along its propagation axis together with a matched chirped laser pulse. The technology for the envisioned primary beams are currently available through LINACS and CPA respectively. The low energy gradient required on the electron bunch for this Thomson scheme is actually beneficial; it necessitates a long bunch length which reduces the Coulomb forces and allows for higher charge up to several nano-Coulombs. Foreseen advantages for the uncompressed CPA laser pulse are the high repetition rate at which a Thomson source can operate (kHz) coupled with higher wall efficiency because the full energy is available (i.e. no compression losses of tens of percent).

The number of keV photons obtainable with the proposed scheme within a 2% bandwidth can reach up to $10^9 - 10^{10}$ per shot, which can lead up to $10^{12} - 10^{13}$ photons per second.

REFERENCES

- [1] D. Haden *et al.*, “High energy x-ray compton spectroscopy via iterative reconstruction,” *Nucl. Instrum. Methods Phys. Res., Sect. A*, vol. 951, p. 163 032, 2020. doi: 10.1016/j.nima.2019.163032

- [2] Z. Chi, Y. Du, W. Huang, and C. Tang, "Linearly polarized X-ray fluorescence computed tomography based on a Thomson scattering light source: a Monte Carlo study," *J. Synchrotron Radiat.*, vol. 27, no. 3, pp. 737–745, 2020. doi:10.1107/S1600577520003574
- [3] F. Schwab *et al.*, "Comparison of contrast-to-noise ratios of transmission and dark-field signal in grating-based x-ray imaging for healthy murine lung tissue," *Z. Med. Phys.*, vol. 23, no. 3, pp. 236–242, 2013, Schwerpunkt: Röntgenbasierte Phasenkontrast Bildgebung. doi:10.1016/j.zemedi.2012.11.003
- [4] A. Zilges, D. Balabanski, J. Isaak, and N. Pietralla, "Photonuclear reactions—from basic research to applications," *Prog. Part. Nucl. Phys.*, vol. 122, p. 103 903, 2022. doi:10.1016/j.pnpnp.2021.103903
- [5] V. Petrillo *et al.*, "State of the art of high-flux Compton/Thomson x-rays sources," *MDPI Appl. Sci.*, vol. 13, no. 2, 2023. doi:10.3390/app13020752
- [6] G. A. Krafft, B. Terzić, E. Johnson, and G. Wilson, "Scattered spectra from inverse Compton sources operating at high laser fields and high electron energies," *Phys. Rev. Accel. Beams*, vol. 26, p. 034 401, 2023. doi:10.1103/PhysRevAccelBeams.26.034401
- [7] M. A. Valialshchikov, V. Y. Kharin, and S. G. Rykovanov, "Narrow bandwidth gamma comb from nonlinear Compton scattering using the polarization gating technique," *Phys. Rev. Lett.*, vol. 126, p. 194 801, 2021. doi:10.1103/PhysRevLett.126.194801
- [8] T. Xu, M. Chen, F.-Y. Li, L.-L. Yu, Z.-M. Sheng, and J. Zhang, "Spectrum bandwidth narrowing of Thomson scattering X-rays with energy chirped electron beams from laser wakefield acceleration," *Appl. Phys. Lett.*, vol. 104, no. 1, 2014, 013903. doi:10.1063/1.4861594
- [9] B. H. Schaap, T. D. C. de Vos, P. W. Smorenburg, and O. J. Luiten, "Photon yield of superradiant inverse Compton scattering from microbunched electrons," *New Journal of Physics*, vol. 24, no. 3, p. 033 040, 2022. doi:10.1088/1367-2630/ac59eb
- [10] B. H. Schaap, P. W. Smorenburg, and O. J. Luiten, "Isolated attosecond x-ray pulses from superradiant Thomson scattering by a relativistic chirped electron mirror," vol. 12, p. 19 727, 2022. doi:10.1038/s41598-022-24288-1
- [11] M. Ruijter, V. Petrillo, and M. Zepf, "Decreasing the bandwidth of linear and nonlinear Thomson scattering radiation for electron bunches with a finite energy spread," *Phys. Rev. Accel. Beams*, vol. 24, p. 020 702, 2021. doi:10.1103/PhysRevAccelBeams.24.020702
- [12] V. Petrillo *et al.*, "A laser frequency transverse modulation might compensate for the spectral broadening due to large electron energy spread in Thomson sources," *MDPI Photonics*, vol. 9, no. 2, 2022. doi:10.3390/photonics9020062
- [13] A. Bacci *et al.*, "Electron Linac design to drive bright Compton back-scattering gamma-ray sources," *J. Appl. Phys.*, vol. 113, no. 19, 2013, 194508. doi:10.1063/1.4805071
- [14] Y. Lurie, A. Friedman, and Y. Pinhasi, "Single pass, the spectral range free-electron laser driven by a photocathode hybrid rf linear accelerator," *Phys. Rev. ST Accel. Beams*, vol. 18, p. 070 701, 2015. doi:10.1103/PhysRevSTAB.18.070701
- [15] A. Bartnik, C. Gulliford, I. Bazarov, L. Cultera, and B. Dunham, "Operational experience with nanocoulomb bunch charges in the Cornell photoinjector," *Phys. Rev. ST Accel. Beams*, vol. 18, p. 083 401, 2015. doi:10.1103/PhysRevSTAB.18.083401
- [16] N. Balal, V. L. Bratman, A. Friedman, and Y. Lurie, "Capabilities of Terahertz Super-Radiance from Electron Bunches Moving in Micro-Undulators," in *Proc. FEL'19*, Hamburg, Germany, Aug. 2019, pp. 517–520. doi:10.18429/JACoW-FEL2019-WEP086
- [17] I. Petrushina *et al.*, "High-brightness continuous-wave electron beams from superconducting radio-frequency photoemission gun," *Phys. Rev. Lett.*, vol. 124, p. 244 801, 2020. doi:10.1103/PhysRevLett.124.244801
- [18] Z. Huang, Y. Ding, and C. B. Schroeder, "Compact x-ray free-electron laser from a laser-plasma accelerator using a transverse-gradient undulator," *Phys. Rev. Lett.*, vol. 109, p. 204 801, 2012. doi:10.1103/PhysRevLett.109.204801
- [19] F. Jafarinia, "Studies on experiments and free-electron laser concepts with a transverse gradient undulator," Ph.D. dissertation, 2021. doi:10.3204/PUBDB-2021-04248
- [20] A. Jullien *et al.*, "Carrier-envelope-phase stable, high-contrast, double chirped-pulse-amplification laser system," *Opt. Lett.*, vol. 39, no. 13, p. 3774, 2014. doi:10.1364/ol.39.003774
- [21] M. Pittman, S. Ferré, J.-P. Rousseau, L. Notebaert, J.-P. Chambaret, and G. Chériaux, "Design and characterization of a near-diffraction-limited femtosecond 100-tw 10-hz high-intensity laser system," *Appl. Phys. B*, vol. 74, pp. 529–535, 2002. doi:10.1007/s003400200838
- [22] M. Narimousa, M. Sabaeian, S. M. M. Ghahfarrokhi, and O. Panahi, "Second-order interferometric autocorrelation for measuring group velocity dispersion and pulse broadening of femtosecond pulses," *Appl. Opt.*, vol. 57, no. 18, pp. 5011–5018, 2018. doi:10.1364/AO.57.005011
- [23] A. Debus *et al.*, "Circumventing the dephasing and depletion limits of laser-wakefield acceleration," *Phys. Rev. X*, vol. 9, p. 031 044, 2019. doi:10.1103/PhysRevX.9.031044
- [24] T. Ziegler *et al.*, "Proton beam quality enhancement by spectral phase control of a PW-class laser system," *Sci. Rep.*, vol. 11, no. 1, p. 7338, 2021. doi:10.1088/0034-4885/75/5/056401
- [25] M. Ruijter, "Radiation effects for the next generation of synchrotron radiation facilities," Ph.D. dissertation, 2022. https://iris.uniroma1.it/retrieve/e383532e-ce2a-15e8-e053-a505fe0a3de9/Tesi_dottorato_Ruijter.pdf
- [26] Y. Ding *et al.*, "Beam shaping with a passive linearizer at the lcls-ii for high-current operation," <https://www-lcls.slac.stanford.edu/web/technotes/LCLS-II-TN-18-02.pdf>